Assembly of the *Drosophila* 26 S proteasome is accompanied by extensive subunit rearrangements

Éva KURUCZ*, István ANDÓ*, Máté SÜMEGI*, Harald HÖLZL†, Barbara KAPELARI†, Wolfgang BAUMEISTER† and Andor UDVARDY*[1]

*Biological Research Center of the Hungarian Academy of Sciences, P.O. Box 521, H-6701 Szeged, Hungary, and †Max Planck Institute of Biochemistry, Au Klopferspitz 18a, D-82152 Martinsried, Germany.

The subunit contacts in the regulatory complex of the *Drosophila* 26 S proteasome were studied through the cross-linking of closely spaced subunits of the complex, and analysis of the cross-linking pattern in an immunoblot assay with the use of subunit-specific monoclonal antibodies. The cross-linking pattern of the purified 26 S proteasome exhibits significant differences as compared with that of the purified free regulatory complex. It is shown that the observed differences are due to extensive rearrangement of the subunit contacts accompanying the assembly of the 26 S proteasome from the regulatory complex and the 20 S proteasome. Cross-linking studies and electron microscopic examinations revealed that these changes are reversible and follow the assembly or the disassembly of the 26 S proteasome. Although the majority of the changes observed in the subunit contacts affected the hexameric ring of the ATPase subunits, the alterations extended over the whole of the regulatory complex, affecting subunit contacts even in the lid subcomplex. Changes in the subunit contacts, similar to those in the regulatory complex, were detected in the 20 S proteasome. These observations indicate that the assembly of the 26 S proteasome is not simply a passive docking of two rigid subcomplexes. In the course of the assembly, the interacting subcomplexes mutually rearrange their structures so as to create the optimal conformation required for the assembly and the proper functioning of the 26 S proteasome.

Key words: cross-linking, regulatory complex, 20 S proteasome, subunit conformational change.

INTRODUCTION

Short-lived or misfolded proteins are recognized and postsynthetically modified by an enzymic cascade which marks the selected protein with a multi-ubiquitin tag (for reviews see [1,2]). Multi-ubiquitinated proteins are selectively recognized and eliminated by a large multiprotein protease complex, the 26 S proteasome (for reviews see [3,4]). This is composed of a barrel-shaped catalytic core, the 20 S proteasome, and two regulatory complexes attached to the bases of the barrel. In contrast with the 26 S proteasome, its catalytic core can efficiently degrade non-ubiquitinated proteins, indicating that the selectivity of the enzyme is ensured by the regulatory complexes. This assumption is supported by the observation that the only subunit known to be able to selectively recognize and bind multiubiquitin chains in an *in vitro* assay, is a component of the regulatory complex [5–10]. Three nanocompartments are located inside the 20 S proteasome, connected to each other by a narrow central channel. The orifices of this channel, which are the entry sites of substrate proteins [11], are situated at the bases of the barrel in the *Thermoplasma acidophilum* 20 S proteasome [12]. In the crystal structure of the *Saccharomyces cerevisiae* 20 S proteasome, however, these orifices are missing, suggesting that the channel may be gated in eukaryotes [13,14]. As a consequence of the narrowness of the central channel, the active centres in the central nanocompartment of the catalytic core are inaccessible to folded proteins. Protein unfolding is probably the second most important function of the regulatory complexes. The chaperone-like activity of the regulatory complex may be responsible for protein unfolding [15,16]. The 26 S proteasome is an ATP-dependent protease. There are at least two independent steps in the catalytic cycle of the proteasome which require ATP hydrolysis: the assembly of the 26 S proteasome from the regulatory complexes and the 20 S proteasome, and most probably the unfolding of the substrate proteins. The six ATPase subunits present in the regulatory complex [17–20] may perform the ATP hydrolysis required in these processes. Although no direct experimental evidence is available, it is reasonable to suppose that the feeding of the unfolded protein into the gated central channel of the 20 S proteasome is also an energy-dependent function of the regulatory complex.

The multifaceted functions of the regulatory complex, and the multitude of substrate proteins upon which all these functional steps must be executed, explain the complex subunit composition of the regulatory complex. In the human [18], yeast [20] and *Drosophila* [21] regulatory complexes, at least 17 highly conserved subunits have been identified. Six of these subunits belong to a special class of ATPases (the AAA-ATPases), which most probably form a hexameric ring and stack to the external α-ring of the 20 S proteasome. These ATPase subunits have a common structural role in forming a hexameric ring capable of docking precisely to the base of the 20 S proteasome. Besides this structural role, the individual ATPase subunits must perform distinct functions, because the phenotypic defects of the different ATPase mutants in yeast are strikingly varied [22]. Our knowledge of the functions of the 11 conserved non-ATPase subunits is very limited. Although S5a/Rpn 10/p54 (the nomenclature for the human, yeast and *Drosophila* regulatory complex subunits is

Abbreviations used: 16-BAC, benzyldimethyl-n-hexadecylammonium chloride; DSS, disuccinyl suberate; mAb, monoclonal antibody; 2D, two-dimensional; msa, multivariate statistical analyses; mra, multi-reference analysis; AMP-PNP, adenosine 5′-[β,γ-imido]triphosphate.

[1] To whom correspondence should be addressed (e-mail udvardy@nucleus.szbk.u-szeged.hu).

Table 1 Human and yeast homologues of the *Drosophila* regulatory complex subunits and the antibody panel against the *Drosophila* subunits

Drosophila	Human	Yeast	Antibody
110	S1	Rpn 2	anti-S1 polyclonal
p97	S2	Rpn 1	–
p58	S3	Rpn 3	mAb u6/272
p56	S4	Rpt 2	anti-p56 polyclonal
p55	S5b	Rpn 5	–
p54	S5a	Rpn 10	mAb 439
p50	S6′	Rpt 5	mAb 112
p48A	S6	Rpt 3	mAbs IB8 and 12A1
p48B	S7	Rpt 1	anti-p48B polyclonal
p42A	S10	Rpn 7	mAbs 123 and 243
p42B	S9	Rpn 6	–
p42C	S8	Rpt 6	mAb 9E3
p42D	S10b	Rpt 4	mAb 216
p39A	S11	Rpn 9	mAb 50
p39B	S12	Rpn 8	–
p37A	–	–	–
p37B	S13	Rpn 11	–

given in Table 1) is the only subunit which can specifically recognize and bind multi-ubiquitin chains *in vitro*, its role in substrate recognition is still debated in view of the observation that deletion of this subunit in yeast is not lethal, and has only a mild phenotype [10]. Deletion of this subunit in *Physcomitrella patens*, however, causes developmental arrest [23], and the polyubiquitin-binding site of the fission yeast homologue is essential when the S14/Rpn 12/p30 subunit is compromised [24]. The second well-defined enzymic function of the regulatory complex, reprocessing of the ubiquitin moieties from multi-ubiquitinated proteins before the degradation step, has been attributed to a unique subunit in the *Drosophila* regulatory complex [21], and a similar activity has been shown to be associated with the bovine [25], yeast [26] and rabbit [27] regulatory complexes.

Two other experimental approaches have been widely used to decipher the functions of the individual subunits or to establish a structure–function correlation within the regulatory complex. Mutational analysis of the subunits of the regulatory complex provided important functional information (reviewed in [4]), while the topology of the regulatory complex was approached through the study of subunit interactions with different biochemical techniques (reviewed in [28]).

As an extension of the analysis of subunit interactions, we studied the structure of the free regulatory complex and the 26 S proteasome by covalently cross-linking the closely spaced subunits within these multi-protein complexes by bifunctional protein cross-linkers. A panel of monoclonal and polyclonal antibodies specific for the different subunits of the *Drosophila* regulatory complex was generated and used to analyse the cross-linking patterns. These studies enabled us to demonstrate an extensive subunit rearrangement within the regulatory complex in the course of the assembly of the 26 S proteasome from its constituent subcomplexes.

EXPERIMENTAL

Purification of the 26 S proteasome from *Drosophila* embryos

An embryonic extract prepared as described previously [29] was the starting material of two distinct purification procedures. The extract was preincubated in the presence of 1 mM ATP and 1 mM dithiothreitol at 25 °C for 40 min. All the buffers in the subsequent purification steps contained 1 mM ATP. In the conventional purification procedure [29], hydroxylapatite, DEAE-cellulose (DE 52) and Superose 6 chromatographic purification steps were applied. To ensure the complete removal of proteins non-specifically associated with the proteasome, a second purification procedure was developed. In this procedure, hydroxylapatite chromatography was followed by three high-resolution chromatographic purification steps. The hydroxylapatite fraction was dialysed against buffer A [20 mM Tris/HCl, pH 7.6, 5 mM $MgCl_2$, 1 mM ATP, 1 mM dithiothreitol and 5 % (v/v) glycerol] containing 100 mM NaCl and loaded on to a Fractogel EMD DEAE (S) high-performance anion-exchange column (Merck, Darmstadt, Gemany). Proteins were eluted with a linear NaCl gradient (100–500 mM in buffer A) and the elution position of the 26 S proteasome was determined by means of a fluorogenic assay [20] with succinyl-Leu-Leu-Val-Tyr-amido-4-methylcoumarin (Bachem Feinchaemikalien AG, Bubendorf, Switzerland) as substrate. Active fractions were dialysed against buffer A containing 100 mM NaCl and purified further on a Fractogel EMD Heparin (S) high-performance column (Merck). Proteins were eluted with a linear NaCl gradient (100–500 mM in buffer A). In the last purification step, active fractions from the heparin column were size-fractionated on a Superose 6 column (Amersham Biosciences, Little Chalfont, Bucks., U.K.) in buffer B (as buffer A, but the Tris/HCl is replaced by Hepes, pH 7.6) containing 100 mM NaCl.

Purification of the free regulatory complex and the 20 S proteasome

Endogenous ATP was depleted from the embryonic extract by preincubation with 0.5 mM 2-deoxy-D-glucose and 1 μg/ml hexokinase (Boehringer Mannheim, Mannheim, Germany) for 40 min at 25 °C. The free regulatory complex and the 20 S proteasome were purified with the second procedure described above, but in the absence of ATP. The elution position of the regulatory complex was determined via an immunodot blot assay, as described previously [29].

Protein gel electrophoresis and immunoblotting

Denaturing SDS/polyacrylamide gels were prepared by standard techniques. The subunits of the purified regulatory complex were separated on two different two-dimensional (2D) gel systems. The benzyldimethyl-n-hexadecylammonium chloride (16-BAC)/SDS/polyacrylamide 2D gel gave much better resolution for certain regulatory complex subunits than did the conventional isoelectric focusing ('IEF')/SDS/polyacrylamide 2D gel system. For 16-BAC/SDS/polyacrylamide 2D gel electrophoresis [30] the subunits of the purified 26 S proteasome were first separated on a 16-BAC/polyacrylamide gel (8.5 %), using a 6 cm wide preparative slot. The gel was fixed in 40 % methanol/10 % acetic acid for 6 h (with repeated changes of the fixer to remove 16-BAC completely). The gel was cut into 3 mm wide strips and stored in the fixer. For the 2D gel electrophoresis, two strips were soaked for 15 min in water, for 15 min in 0.125 M Tris/HCl, pH 6.8, and for 5 min in SDS-sample buffer. To obtain two identical 2D gels, an SDS/polyacrylamide gel (8 %) with two wide preparative slots was prepared, and the strips were loaded into the slots and run as conventional SDS/polyacrylamide gels. One of the identical 2D gels was stained with Coomassie Blue, and the other was used for immunoblotting.

Proteins from 1D or 2D gels were transferred to nitrocellulose membrane, reacted with different subunit-specific monoclonal or polyclonal antibodies and revealed by the enhanced chemiluminescent technique, using horseradish peroxidase ('HRP'-

conjugated second antibodies and the Supersignal-HRP chemiluminescent substrate (Pierce, Rockford, IL, U.S.A.).

Native PAGE was performed on the single gel layer system described by Glickman et al. [20] in the presence or absence of ATP as indicated.

Protein identification by matrix-assisted laser-desorption ionization–time of flight-MS

Protein bands were excised and cleaved directly in the gel with endoproteinase LysC (Boehringer Mannheim). Peptide mass fingerprinting was performed with a Bruker Reflex II matrix-assisted laser-desorption ionization–time of flight mass spectrometer (Bruker-Franzen, Bremen, Germany) equipped with a 337 nm nitrogen laser. One μl of the eluted peptide mixture was applied on to the sample target. After drying at 25 °C, 0.7 μl of the matrix solution (5 mg of α-cyano-4-hydroxycinnamic acid dissolved in 1 ml of acetonitrile/water/trifluoroacetic acid (50:50:0.1, by vol.) was overlaid and dried again at 25 °C. Mass analysis was performed in the positive reflector mode with delayed extraction, at an accelerating voltage of 20 kV and a reflector voltage of 22.8 kV, with a deflection cut off mass of 400. Typically 100–150 shots were accumulated. The peptide masses found were used in a database search, using the program MSFIT.

Protein cross-linking

Purified 26 S proteasome or the free regulatory complex was incubated in the presence of 100 μM disuccinyl suberate (DSS, Pierce) for 15 min at 25 °C. The reaction was quenched by the addition of 20 mM glycine. Proteins were precipitated with ice-cold trichloroacetic acid (10 % final concentration), and the precipitate was washed with cold acetone, dried and dissolved in SDS-sample buffer. The cross-linking pattern was analysed by an immunoblotting technique, with subunit-specific antibodies.

Subunit-specific monoclonal antibodies were raised in mice immunized with the purified regulatory complex. Hybridoma cell lines were selected by standard procedures [31]. The subunit recognized by a monoclonal antibody was identified in an immunoblot assay after separation of the subunits of the purified regulatory complex by 2D gel electrophoresis. Comparison of a Coomassie Blue-stained 2D gel with the immunoblot pattern of identical 2D gels unequivocally identified the subunit recognized by the antibody. Polyclonal antibodies were generated in rabbits by using recombinant regulatory complex subunits expressed in *Escherichia coli*.

Immunoprecipitation

Subunits of the cross-linked 26S proteasomes were dissociated by boiling for 5 min in 2.5 % (w/v) SDS. After the addition of 20 volumes of 1 % (v/v) Triton X-100 in PBS, mAb-charged Protein G–Sepharose beads were added and incubated at 4 °C for 10 h with continuous shaking. The beads were washed several times in 0.1 % Triton X-100 in PBS, the proteins bound by the antibody-charged beads were eluted by boiling the beads in SDS-sample buffer and analysed in an immunoblot assay.

Electron microscopy and image processing

The method of embedding single particles in unsupported ammonium molybdate-containing vitreous ice films was adopted with some modifications [32]. In brief, 5 μl of the purified *Drosophila* 26 S proteasome solution (approx. 400 μg/ml) was applied to a carbon grid and washed twice on the grid with 20 mM Tris/HCl buffer, pH 7.2, containing 2 mM ATP. A droplet of an aqueous solution of 16 % (v/v) ammonium molybdate, 10 mM $MgCl_2$, either with or without 2 mM ATP, was applied for 5 s. Excess liquid was then blotted away, the grid was plunged into liquid ethane and then transferred to liquid nitrogen.

Electron microscopy was carried out under low-dose cryo conditions, using a CM200 transmission electron microscope (Philips, Best, The Netherlands) equipped with a field emission gun, which was operated at 160 kV accelerating voltage. Images were recorded digitally (Photometrix slow scan CCD, 2048 × 2048 pixels) at 2 μm defocus and a total magnification of × 34400 (corresponding to a pixel size of 0.407 nm at the CCD level).

Image processing steps were carried out on a Silicon graphics workstation using the 'EM' program package. All electron micrographs were low-pass filtered for further processing (the contrast transfer function was cut off at the first zero at 2.5 nm^{-1}). For structural investigation 1640 different 96 × 96 sub-frames of individual particles were extracted and normalized to the zero mean. Two-dimensional image analysis started with five cycles of rotational and translational alignment based on cross correlation techniques [33], with the first reference obtained by aligning 20 randomly selected particles. As the particles yield a variety of 2D views, the appropriate method for image analysis was to apply a series of alternating multivariate statistical analyses (msa) [34] and multi-reference analysis (mra) steps. For further analysis the collected dataset was subjected to msa followed by classification into 20 classes according to the 20 most significant eigenimages. The means of the most prominent classes were used as a set of independent reference images for subsequent mra. Thereafter msa and classification were repeated and the most homogeneous subclasses were subjected separately to rotational and translational alignment relative to the corresponding subclass mean as a reference. Within each subclass msa and classification was carried out.

RESULTS

Characterization of the antibodies developed against *Drosophila* regulatory complex subunits

To study the topology of subunits within the regulatory complex of the *Drosophila* 26 S proteasome, a panel of subunit-specific monoclonal (or polyclonal) antibodies was generated. To identify the subunit recognized by the different antibodies, the subunits of the purified regulatory complex were separated on two identical 16-BAC/SDS/polyacrylamide 2D gels; one of them was stained with Coomassie Blue, and the other was used for immunoblot assay. The spot recognized by an antibody was cut from the Coomassie-Blue-stained gel and identified by protein microsequencing (Figure 1B and Table 1). As shown in Figure 1(A), the majority of the regulatory complex subunits are represented in our antibody library. With the exception of mAb 12A1, all the antibodies recognized a single subunit of the regulatory complex, and a single protein band reacted with these antibodies in a total *Drosophila* embryonic extract (results not shown).

Protein microsequencing revealed that subunit p48A is present in two distinct spots (Figure 1B). The upper spot proved to be a mixture of subunits p50 and p48A, while all the peptides derived from the lower spot corresponded to genuine p48A sequences. This indicates that p48A is present in two electrophoretically distinct forms, probably as a consequence of a postsynthetic modification. mAb 12A1 gave a strong signal on the upper spot and a weak signal on the lower spot (Figure 1E). The upper spot (a mixture of p50 and p48A) also reacted with mAb 112 (results not shown). As recombinant p50 protein expressed in *Escherichia coli* did not react with mAb 12A1, but reacted strongly with mAb 112 (results not shown), mAb 12A1 must react with subunit p48A, and recognizes both electrophoretic variants of

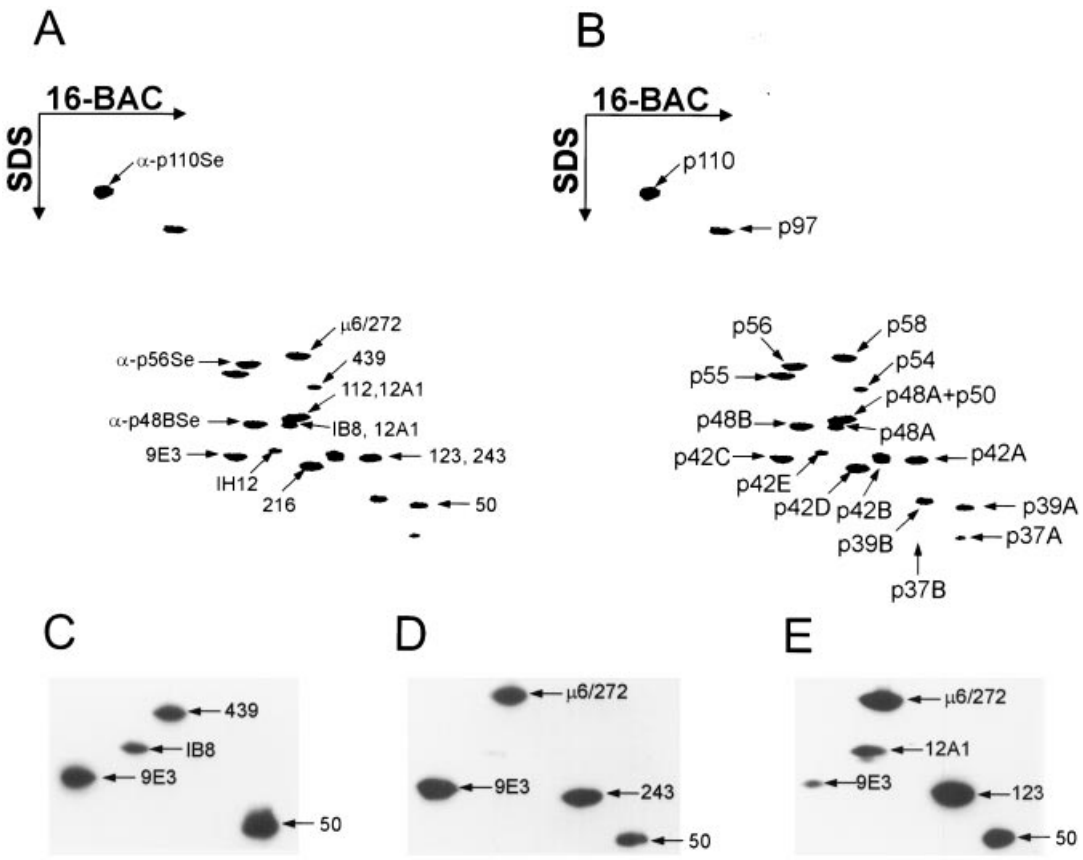

Figure 1 16-BAC/SDS/polyacrylamide 2D gel pattern of the regulatory complex

The subunits of the purified regulatory complex were separated on two identical 16-BAC/SDS/polyacrylamide 2D gels. The first gel was stained with Coomassie Blue and the spots were excised for protein microsequencing, while the second gel was blotted to nitrocellulose and reacted with different combinations of subunit-specific antibodies. (**A**) Subunit specificity of the monoclonal and polyclonal antibodies. (**B**) Identification of the subunits of the regulatory complex by protein microsequencing. The nomenclature of the subunits and their yeast and human homologues is described in Table 1. (**C**) mAb IB8 recognizes only one electrophoretic variant of p48A. For alignment mAbs 439, 9E3 and 50 were also included in the reaction. (**D**) mAb 123 and (**E**) mAb 243 recognize the same subunit of the regulatory complex (p42A). For alignment mAbs μ6/272, 9E3 and 50 were also included in the reaction. (**E**) mAb 12A1 recognizes both electrophoretic variants of p48A. For comparison with (**C**) spots recognized by mAbs 9E3 and 50 can help alignment.

p48A (albeit with different intensities). mAb IB8 is another p48A-specific antibody, but in contrast with mAb 12A1, it recognizes only the lower spot, which reacts weakly with mAb 12A1 (Figures 1C and 1E).

The spatial arrangement of the regulatory complex subunits is changed significantly following the disassembly of the 26 S proteasome

Closely spaced subunits within a multi-protein complex can be covalently cross-linked with bifunctional protein cross-linkers. The cross-linked products can readily be revealed in an immunoblot assay with subunit-specific monoclonal antibodies. To optimize the concentration of the cross-linker, the purified regulatory complex was incubated with increasing concentrations of DSS (a homobifunctional amino group-specific cross-linker) and the formation of cross-linking products was tested in an immunoblot assay with mAb 112. As shown in Figure 2(A), there was no significant change in the overall character of the cross-linking pattern within the DSS concentration range tested. At 100 mM DSS, all the details of the cross-linking pattern were clearly visible. This is the standard cross-linker concentration used in the experiments shown in Figures 2(B)–2(M).

The cross-linking studies revealed that the disassembly of the 26 S proteasome was accompanied by extensive subunit re-arrangements. This conclusion is based on the observation that the cross-linking pattern of the purified 26 S proteasome exhibits significant differences compared with that of the purified free regulatory complex. As revealed in Figures 2(B)–2(H), the most extensive rearrangements occurred along the ATPase subunits. mAb 9E3, which recognizes the ATPase subunit p42C (Figure 1C), detects a very broad and intensive cross-linking product in the 26 S proteasome, while for the free regulatory complex the intensity of this band is dramatically less and only a faint, closely spaced duplex is visible in this position (Figure 2B). There are two additional faint bands in the upper region of the gel for the 26 S proteasome, while for the free regulatory complex these bands are slightly displaced downward and a third, more intensive band appears, which is almost completely missing from the pattern for the assembled 26 S proteasome. Doubling the cross-linker concentration did not eliminate these differences (results not shown), indicating that the change in the pattern reflects a genuine conformational rearrangement of the subunit within the regulatory complex. The disassembly-dependent conformational changes are even more complicated for another ATPase subunit, p48A. The protein microsequencing following 2D gel separation

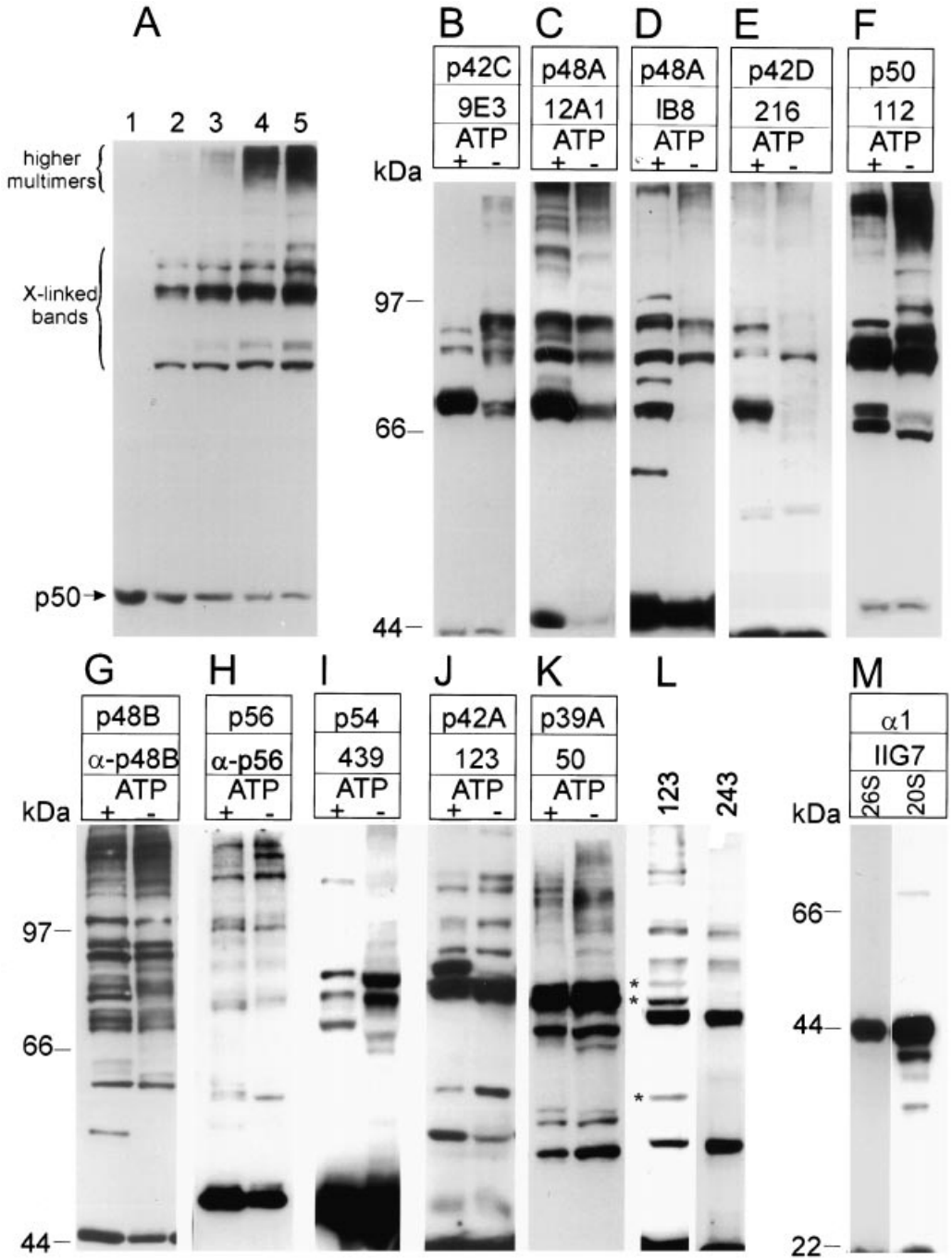

Figure 2 Cross-linking patterns revealed by different subunit-specific mAbs in the 26 S proteasome and the free regulatory complex

(**A**) The purified free regulatory complex was incubated with increasing concentrations of DSS and the extent of cross-linking was followed by immunoblotting with mAb 112. The non-cross-linked subunit of p50, the cross-linked dimers (X-linked bands) and the cross-linked higher multimers are marked. Lane 1, 0 mM DSS; lane 2, 25 mM DSS; lane 3, 50 mM DSS; lane 4, 100 mM DSS; lane 5, 200 mM DSS. (**B–J**) Cross-linking patterns of the 26 S proteasome (lane ATP+) and the free regulatory complex (lane ATP−) revealed with different regulatory complex subunit-specific antibodies: (**B**) p42C, 9E3; (**C**) p48A, 12A1; (**D**) p48A, IB8; (**E**) p42D, 216; (**F**) p50, 112; (**G**) p48B, α-p48B; (**H**) p56, α-p56; (**I**) p54, 439; (**J**) p42A, 123; (**K**) p39A, 50. (**L**) Cross-linking pattern of the 26 S proteasome visualised with mAb 123 and mAb 243. (**M**) Cross-linking patterns of the 26 S proteasome (lane 26S) and the free 20 S proteasome (lane 20S) visualized with the 20 S proteasome-specific mAb IIG7.

of the regulatory complex subunits unequivocally proved that subunit p48A is present in two distinct forms. It is reasonable to suppose that the slower electrophoretic variant corresponds to a postsynthetically modified form of the subunit. mAbs 12A1 and IB8 recognize the slower and the faster electrophoretic variants, respectively. The cross-linking pattern generated by mAb IB8 is significantly different from that with mAb 12A1. The appearance of two new bands detected only with mAb IB8 (Figures 2C and 2D) suggests that the presumed postsynthetic modification may induce rearrangements in the conformation of subunit p48A.

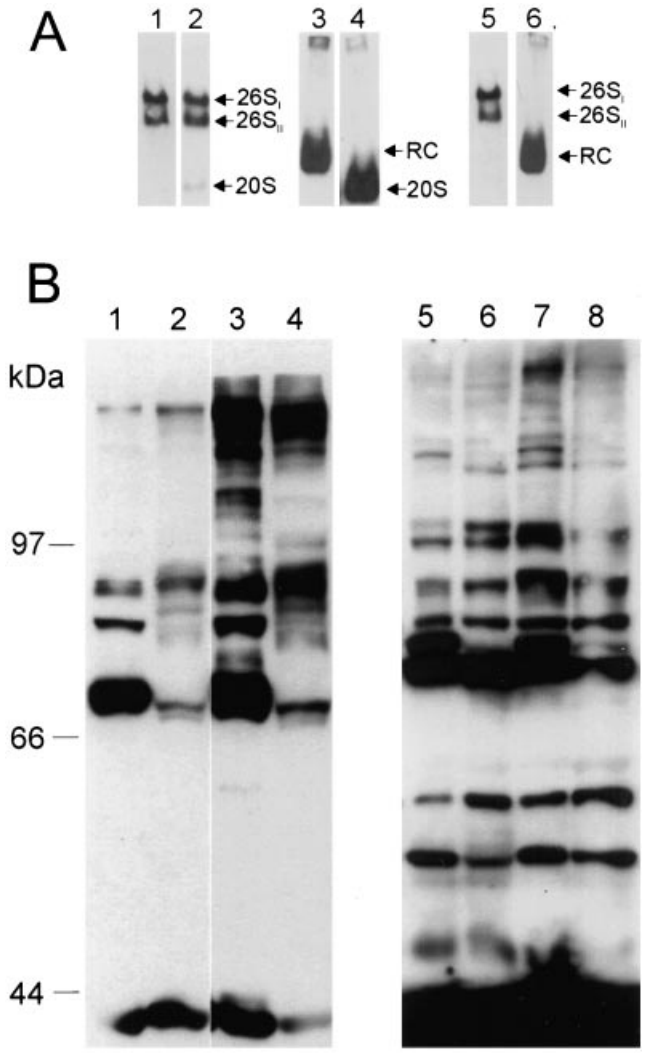

Figure 3 Reversible assembly-disassembly of the 26 S proteasome is accompanied by extensive subunit rearrangements

(**A**) The 26 S proteasome present in the hydroxylapatite pool was fractionated by native PAGE in the presence of ATP, blotted and revealed with an anti-regulatory complex antibody (lane 1) or an anti-20 S proteasome antibody (lane 2). After enzymic ATP depletion, the same hydroxylapatite fraction was analysed on a native PAGE prepared without ATP. Lane 3, reaction with an anti-regulatory complex antibody; lane 4, reaction with an anti-20 S proteasome antibody. Lane 5, the ATP-depleted hydroxylapatite fraction was incubated in the presence of an excess of ATP and an ATP regenerating system (2 mM ATP, 50 mM creatine phosphate with creatine phosphokinase) and analysed as described for lane 1. Lane 6, the ATP-depleted hydroxylapatite fraction was incubated in the presence of AMP-PNP. (**B**) Cross-linking patterns in the hydroxylapatite fraction (lanes 1 and 5), in the ATP-depleted hydroxylapatite fraction (lanes 2 and 6), in the ATP-depleted hydroxylapatite fraction, after incubation in the presence of ATP and an ATP regenerating system (lanes 3 and 7) and in the ATP-depleted hydroxylapatite fraction after incubation with a non-hydrolysable ATP analogue (AMP-PNP) (lanes 4 and 8). The cross-linking pattern was analysed with mAb 9E3 (lanes 1–4) or mAb 123 (lanes 5–8).

The cross-linking patterns detected with mAbs 12A1, 9E3 and 216, and the changes observed in these patterns following the disassembly of the 26 S proteasome are very similar, suggesting the close proximity of the ATPase subunits p42C, p42D and p48A within the regulatory complex (Figures 2B, 2C, 2E, and see below).

mAb 112, which reacts with the fourth ATPase subunit of the *Drosophila* regulatory complex (p50), recognizes two broad, multi-band masses of cross-linked products. The arrangement of these bands demonstrates a characteristic displacement during the disassembly process (Figure 2F).

The character of the cross-linking pattern and its change following the disassembly are completely different for the fifth and sixth ATPase subunits, p56 and p48B (Figures 2G and 2H). The broad ladder of cross-linked bands indicates that these subunits form a multitude of contacts, and the disassembly induces only minor rearrangements in the protein–protein interactions between these subunits.

The assembly-dependent rearrangement of the multi-ubiquitin chain-binding subunit p54 is shown in Figure 2(I). No changes were observed with a mAb developed against subunit p110, the other non-ATPase subunit of the base complex (results not shown).

Although the cross-linking pattern of the 26 S proteasome and that of the free regulatory complex were almost identical with mAb 50, which recognizes the regulator lid subunit p39A (Figure 2K), the subunit rearrangement following the disassembly of the proteasome is not confined merely to the base of the regulatory complex. A very prominent new assembly-dependent band appears in the cross-linking pattern of the lid subunit p42A with mAb123 (Figure 2J).

Two different monoclonal antibodies (mAb 123 and mAb 243) recognize subunit p42A (Figures 1D and 1E). The cross-linking patterns detected with these antibodies for the free regulatory complex and for the 26 S proteasome are very similar, but definitely not identical. Three prominent bands (denoted by * in Figure 2L) detected with mAb 123 are completely missing for the pattern obtained with mAb 243. In repeated protein microsequencing experiments, all the peptides generated from the spot which corresponds to p42A did conform to genuine p42A sequences, indicating that a single polypeptide is present in this spot. The differences in the cross-linking patterns suggest that the p42A subunit is present in two different conformations, which are recognized selectively by these monoclonal antibodies.

In view of the extent of the assembly-dependent subunit rearrangements within the regulatory complex, it was of interest to test the rigidity of the catalytic core during the assembly. The only 20 S proteasome-specific mAb that we have tested (mAb IIG7, which recognizes the α1 subunit of the catalytic core) revealed characteristic differences in the cross-linking pattern of the 26 S proteasome and that of the free 20 S proteasome (Figure 2M). The results with mAb IIG7 suggest that, at least in the α-ring of the 20 S proteasome, the disassembly induces changes in the conformations of the subunits.

The assembly of the 26 S proteasome is accompanied by extensive subunit rearrangements in the regulatory complex

To prove unequivocally that the changes in the cross-linking patterns described above are not due to a structural disintegration of the regulatory complex in consequence of the purification procedure, but reflect the structural basis of the assembly of the 26 S proteasome, the assembly state, the cross-linking pattern and the proteolytic activity of the proteasome were compared. To minimize the risk of structural disintegration of the regulatory complex, this comparative study was performed following the first chromatographic purification step (hydroxylapatite chromatography, which removes only the large mass of the yolk proteins [29]). Native PAGE combined with immunoblot analysis revealed that, in the hydroxylapatite fraction prepared in the presence of ATP, the 26 S proteasome is fully assembled, and no free regulatory complex is present. In agreement with previous observations [20,21], two distinct electrophoretic variants of the 26 S proteasome can be resolved, which may correspond to the singly-

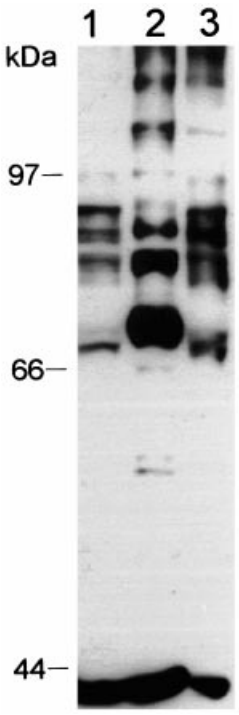

Figure 4 ATP does not induce structural changes in the free regulatory complex

Purified regulatory complex was incubated in the presence (lane 1) or absence (lane 3) of 1 mM ATP and cross-linked under standard conditions. Purified 26 S proteasome cross-linked under the same conditions is shown in lane 2 as a control. The immunoblot was developed with mAb 9E3.

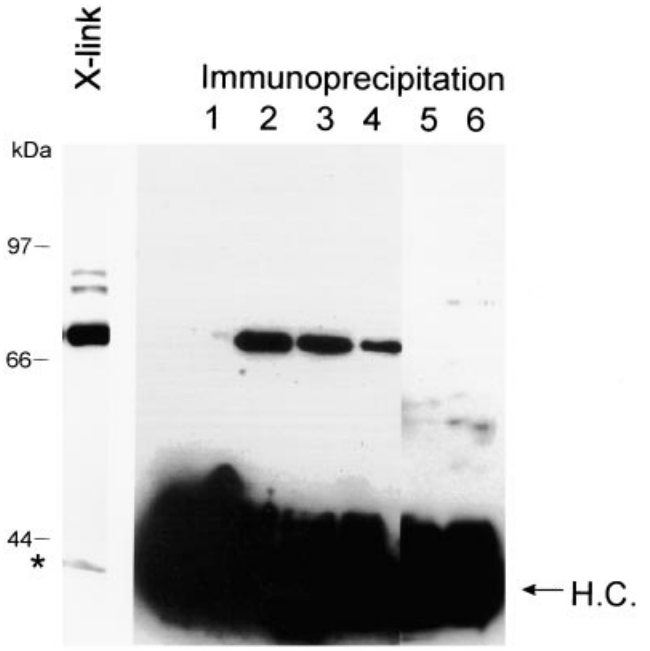

Figure 5 Identification of cross-linked subunits by immunoprecipitation

Cross-linked 26 S proteasomes were boiled in 2.5% SDS and immunoprecipitated with mAbs9E3 (lane 2), 12A1 (lane 3), 216 (lane 4), or with anti-p48B (lane 5) and anti-p56 (lane 6) antibodies. In lane 1 a control immunoprecipitation was done with an indifferent mAb. A cross-linked 26 S proteasome sample (X-link) and immunoprecipitated proteins were separated by SDS/PAGE (7% gel) and analysed in an immunoblot assay with mAb 9E3. The large mass of immunoglobulin heavy chain (H. C., marked by arrow) conceals the immunoprecipitated non-cross-linked subunits (marked by asterisk).

capped and doubly-capped forms of the 26 S proteasome [20,21]. The identity of the immunoblot patterns with anti-regulatory complex and anti-20 S proteasome antibodies indicates that both forms correspond to 26 S proteasome molecules (Figure 3A, lanes 1 and 2). Free 20 S proteasome is present in this fraction in only trace amounts. Following enzymic ATP depletion, the 26 S proteasome dissociates into free regulatory complex and free 20 S proteasome, and on a native polyacrylamide gel prepared without ATP these particles can be separated (Figure 3A, lanes 3 and 4). The regulatory complex in this state, however, is functionally fully competent, because the whole amount of the free regulatory complex can be assembled into the 26 S proteasome again by incubation of the fraction with an excess of ATP (Figure 3A, lane 5). Indirect observations indicate that the reassembly of the 26 S proteasome is very fast. When the ATP-depleted hydroxylapatite fraction was analysed on an ATP-containing native polyacrylamide gel, the whole amount of the regulatory complex was found to be assembled into the 26 S proteasome. This indicates that, in the presence of ATP, the first few minutes of the electrophoresis, i.e. before the separation of the regulatory complex and the catalytic core, is sufficient for the assembly (results not shown).

The high selectivity of our monoclonal antibodies permitted the comparison of the cross-linking patterns of the assembled 26 S proteasome and that of the free regulatory complex even in this crude protein extract. The cross-linking pattern of the regulatory complex followed the assembly changes in the proteasome. In the presence of ATP, the cross-linking pattern, analysed with mAbs 9E3 and 123 (specific for subunit p42C of the base subcomplex and subunit p42A of the lid subcomplex, respectively, exhibiting the most characteristic assembly-dependent changes in these subcomplexes), was indistinguishable from that of the highly purified 26 S proteasome (Figure 3B, lanes 1 and 5). ATP depletion induced a profound change in the subunit contacts within the regulatory complex, generating a cross-linking pattern identical with that observed in the purified regulatory complex (Figure 3B, lanes 2 and 6). In agreement with the observation that the dissociated regulatory complex is fully assembly-competent, the 26 S proteasome-specific cross-linking pattern was reformed in the ATP-depleted hydroxylapatite fraction after incubation with an excess of ATP (Figure 3B, lanes 3 and 7). Neither the assembly (Figure 3A, lane 6) nor the changes in the cross-linking pattern (Figure 3B, lanes 4 and 8) could be induced by incubating an ATP-depleted hydroxylapatite fraction with the non-hydrolysable ATP analogue 2 mM adenosine 5′-[β,γ-imido]triphosphate (AMP-PNP). The functional competence of the free regulatory complex present in the ATP-depleted hydroxylapatite fraction is further supported by the observation that assembly of the 26 S proteasome after the addition of an excess of ATP was accompanied by a 73-fold stimulation of the chymotrypsin-like peptidase activity of the proteasome, measured on the succinyl-Leu-Leu-Val-Tyr-amido-4-methylcoumarin fluorogenic peptide (results not shown).

The rearrangement of subunit contacts in the regulatory complex described above is strictly assembly-dependent. No changes were detected in the cross-linking pattern of the purified free regulatory complex preincubated in the presence or absence of ATP (Figure 4). Thus charging the ATPase subunits of the free regulatory complex with ATP does not induce the restruc-

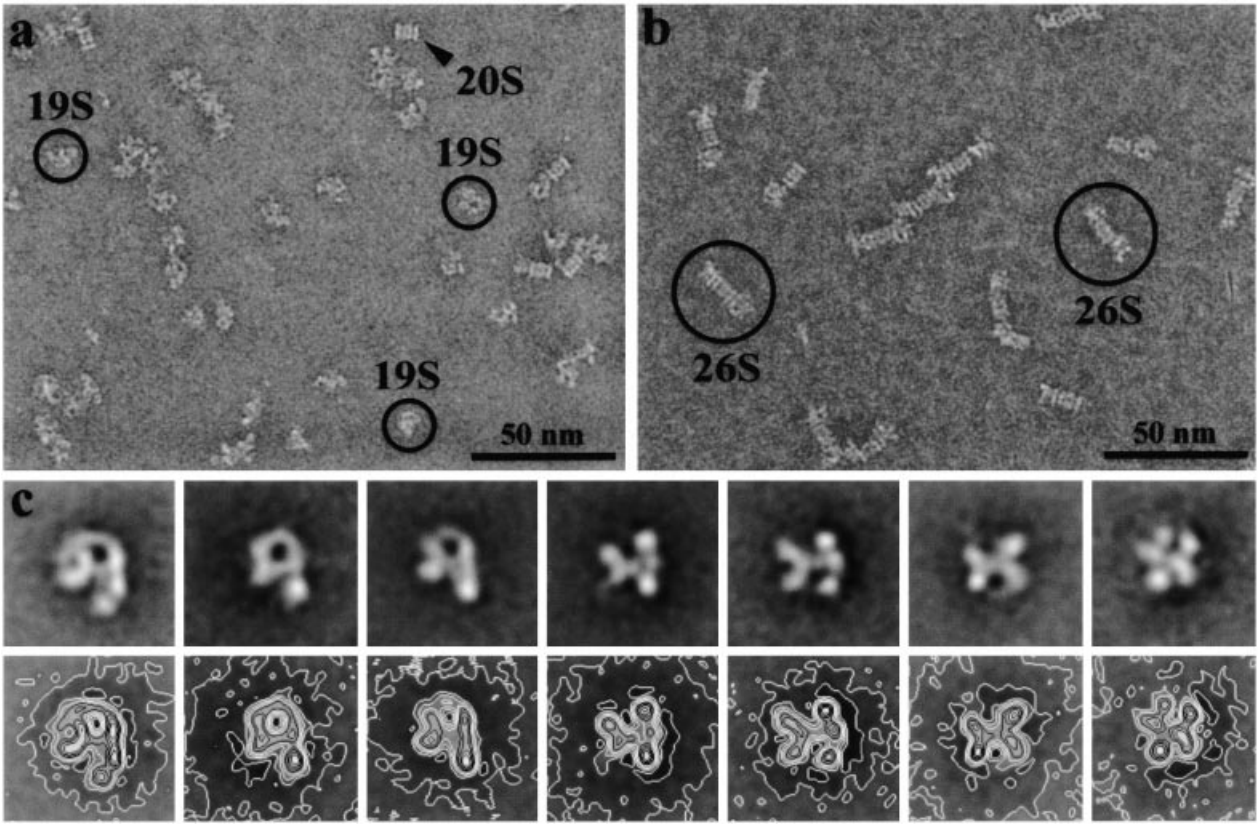

Figure 6 Electron micrograph of the regulatory complex

(**A**) 26 S proteasomes were dissociated by embedding in ATP-depleted unsupported ammonium molybdate-ice film. Dissociated free regulatory complexes are encircled, free 20 S proteasomes are marked with an arrow. (**B**) Intact 26 S proteasomes embedded in ATP-containing unsupported ammonium molybdate-ice film. (**C**) The most prominent characteristic averaged 2D views and corresponding contour line plots of the dissociated 19 S regulatory complexes.

turing of the 26 S proteasome, it is the assembly of the holocomplex which induces the remodelling process.

The similarities of the cross-linking patterns and their changes following the assembly process strongly suggest that three ATPase subunits (p48A, p42D and p42C) have multiple contacts with each other. Immunoprecipitation experiments confirmed these interactions (Figure 5). In this experiment the subunits of the cross-linked 26 S proteasome were dissociated by boiling in the presence of 2.5 % (w/v) SDS and immunoprecipitated with mAbs 9E3 (lane 2), 12A1 (lane 3), 216 (lane 4), or with anti-p48B (lane 5) and anti-p56 (lane 6) antibodies. Immunoprecipitation with an indifferent mAb (developed against soybean leghaemoglobin, lane 1) served as a control. Immunoprecipitated proteins were separated by SDS/PAGE (7 % gel) and probed with mAb 9E3. mAbs 9E3, 12A1 and 216 immunoprecipitated the major cross-linking product detected by mAb 9E3, while only faint reaction was observed with anti-p48B and anti-p56 antibodies.

Electron microscopy reveals structural variances in the regulatory complex immediately after its detachment from the catalytic core

Previous electron microscopy and subsequent digital-image analysis of the isolated regulatory complex has not yielded well defined 2D structures (results not shown). However, several structural variants of the individual 19 S complex were observed, when the 26 S holoenzyme was embedded in ATP-depleted unsupported ammonium-molybdate-ice films. Using this technique, 26 S proteasomes rapidly dissociate into 20 S and intact 19 S complexes. Moreover this technique offers the opportunity to combine the high contrast of negative stain with the possibility of revealing the particles close to their native states, free of constraints imposed by absorption on carbon films. By restricting ammonium molybdate incubation times to 5 sec visualization of the regulatory complex immediately after its detachment from the 20 S core was achieved.

Figure 6 shows electron micrographs of the 26 S proteasomes incubated in ammonium molybdate solution without ATP (Figure 6A), or with 2 mM ATP (Figure 6B), both recorded at 2 μm defocus. When ATP was omitted (Figure 6A) the 26 S proteasomes disassembled into 20 S core and 19 S regulatory complexes, whereas in the presence of ATP (Figure 6B) 26 S proteasomes remained intact and the 20 S core complexes were capped by either one or two 19 S regulatory complexes. Single particle image analysis of the separated 19 S complexes, using mra and repeated msa classification steps, allowed the extraction of distinct classes with resolution better than 25 Å (1 Å $\equiv$ 0.01 nm) according to the Fourier ring criterion. In Figure 6(C) the major class means of the dissociated 19 S complexes are displayed. They clearly vary in diameter, from approx. 22.4–20.4 nm in width, and from 27.7–21.6 nm in length. Classes 1–3 resemble the familiar V- or U-shaped structure of the 19 S complex, as seen in the 26 S holocomplex. The plane basal ring, considered to be constituted by the ATPase subunits, is connected via a 'hinge' region to the outer mass (referred to as lid subcomplex) of the 19 S complex

(left side) and the 20 S core attaches on the right side. The other classes, however differ substantially from this hook-like structure. In classes 4–6 the connection between the putative ATPase ring and the outer masses seems to be connected via a central stalk, whereas the 'hinge region' has disappeared. In class 4 the ring appears to be plane in shape. This is in contrast with the convex shape of the ring in class 5 and a concave shape in class 6, with respect to the outer mass. Class 7 is characterized by five distinct mass centres with no obvious relation of the 3D orientation and projection axis to the previous classes.

A more detailed interpretation of these 2D data is hampered by the difficulty in discriminating between different orientations with respect to the viewing axis, genuine conformational changes and partial dissociation of the particles. Nevertheless the variety of distinct views of the 19 S complex supports the results found with the cross-linking studies on a substantial plasticity of the regulatory complex, and might reflect the remodelling of the 19 S complex during the first seconds following its separation from the 20 S core.

DISCUSSION

Cross-linking studies and electron microscopic observations revealed that the disassembly of the 26 S proteasome, following ATP-depletion, is accompanied by gross structural rearrangement of the regulatory particle. The ATPase subunits that have direct contacts with the 20 S proteasome are most extensively affected. The cross-linking pattern and its change following the disassembly strongly suggest that three ATPase subunits (p48A, p42D and p42C) have multiple contacts with each other. For the assembled 26 S proteasome, there is a broad cross-linked band which reacts with all three subunit-specific mAbs, indicating that these subunits are very closely spaced and can be cross-linked with each other efficiently. Disassembly of the 26 S proteasome results in the displacement of these subunits, and the increased spatial distance between these subunits greatly reduces the efficiency of cross-linking at this contact point. Immunoprecipitation experiments confirmed the close proximity of these subunits (Figure 5). Previous *in vitro* studies with a protein overlay assay [35,36] and likewise biochemical and genetic experiments [37,43] confirm our results: strong interactions were demonstrated between subunits Rpt3/S6b/p48A–Rpt6/S8/p42C and Rpt4/S10bp/p42C–Rpt6/S8/p42D. Our cross-linking approach allowed demonstration not only of the interaction of these subunits, but also of the dynamic changes in these subunit interactions in the course of the disassembly of the 26 S proteasome.

The conformational changes accompanying the disassembly of the 26 S proteasome are not confined to the base of the regulatory complex. A very prominent change was observed in the regulatory lid subunit p42A. The appearance of the new band shown in Figure 2(J) may be due to a direct contact of this subunit with the 20 S proteasome, in which case the assumption that only the base subcomplex has direct contacts with the catalytic core is not valid. It is more probable, however, that the conformational rearrangement of the ATPase subunits generated this new contact. This suggests the neighbouring positions of p42A and the hexameric ATPase ring.

To support these biochemical data, electron microscopy and image analysis were carried out. For the first time 2D structures of the individual 19 S regulatory complex are shown in this study, with resolutions better than 25 Å according to the Fourier ring criterion. Hitherto, only rather indistinct and featureless structures of isolated and purified 19 S complexes have been obtained. The *in situ* disassembly (following ATP depletion) of the 26 S holoenzyme and imaging in unsupported ammonium molybdate-ice films allowed us to capture a number of intermediates following the detachment from the 20 S core. Rapid ATP removal and the concomitant cryofixation of the samples minimize the risk of artefacts. Although the interpretation of these 2D structural data is hampered by the difficulty in discriminating between different orientations with respect to the viewing axis, the observed structural variants probably provide the morphological representation of the remodelling of the regulatory complex following the disassembly of the 26 S proteasome.

The reconstitution of the 26 S proteasomes from highly purified regulatory complex and 20 S proteasomes is inefficient because any assembly factors are removed during the purification [29]. In a partially purified fraction of a *Drosophila* embryonic extract, however, the disassembly and the assembly of the 26 S proteasome is fully reversible. ATP depletion induces the disassembly of the complex, which can be fully reversed by the addition of an excess of ATP. Cross-linking studies of such a partially purified extract revealed that the structural rearrangements described above are not consequences of an artificial structural deterioration of the regulatory complex during the purification procedure. The changes are fully reversible and follow the assembly state of the proteasome, representing the remodelling process required for the assembly and the proper functioning of the 26 S proteasome.

Due to our very limited knowledge of the molecular details of the catalytic cycle of the 26 S proteasome, the interpretation of the structural changes observed by chemical cross-linking is very difficult. The subtle conformational rearrangement in the α-ring of the 20 S proteasome may be associated with the gating of the channel. We can only speculate as to the roles of these rearrangements in the case of the regulatory complex. The spectacular assembly-dependent increase in the extent of cross-linking of subunits p42C, p42D and p48A with each other may represent a compaction of the hexameric ATPase ring. This may be required to match the size and/or the structure of the hexameric ATPase ring to that of the heptameric α-ring of the 20 S proteasome. The energy required for this compaction is provided by the hydrolysis of the ATP, because a non-hydolysable ATP analogue cannot support the increase in the extent of cross-linking of these subunits. The presence of the catalytic core is indispensable for this presumed compaction. In the free regulatory complex, ATP cannot induce the increase in the extent of cross-linking of these ATPase subunits (Figure 4). The physical interaction of the catalytic core and the regulatory complex may provide the physical support for this compaction.

In the case of subunit p48A, indirect evidence suggest that postsynthetic modifications may also induce rearrangements in the subunit contacts (Figures 2C and 2D). The higher eukaryotic homologue of p48A (Rpt3/S6) has been shown to be phosphorylated [38].

It was recently shown that ATP hydrolysis modulates the association of the 26 S proteasome with a multitude of proteasome-interacting proteins [39]. It is reasonable to suppose that for each interaction the regulatory complex must adopt an ideal conformation which is determined and induced by the interacting partner. In this scenario, the plasticity of the regulatory complex is the prerequisite structural basis of the functional redundancy of the proteasome.

The recognition that assembly of the 26 S proteasome is not simply a passive docking of two rigid subcomplexes, but a process accompanied by substantial restructuring of the 26 S proteasome, is the most important message of our results. In the course of the assembly, the interacting subcomplexes mutually

rearrange their structures so as to create the optimal conformation required for the assembly and the proper functioning of the 26 S proteasome.

Recently the subunit interactions in the *Caenorhabditis elegans* and the *Saccharomyces cerevisiae* 26 S proteasome have been studied by the yeast two-hybrid technique [40–42]. Several subunit interactions, undetected by previous biochemical and genetic approaches, have been revealed. The interaction map generated by the yeast two-hybrid technique is very detailed, but provides only a static picture of potential subunit interactions. The cross-linking approach, used in this study, allowed an insight into the dynamic changes of subunit interactions during the assembly of the 26 S proteasome. These observations indicate that several different experimental approaches will be required to map all the subunit contacts in the proteasome, before the crystal structure of this particle is solved.

This work was supported by the National Scientific Research Fund (OTKA T29207, T35074 and T31856).

REFERENCES

1 Hershko, A. and Ciechanover, A. (1998) The ubiquitin system. Annu. Rev. Biochem. **67**, 425–479
2 Ciechanover, A. (1998) The ubiquitin-proteasome pathway: on protein death and cell life. EMBO J. **17**, 7151–7160
3 Baumeister, W., Walz, J., Zühl, F. and Seemüller, E. (1998) The proteasome: paradigm of a self-compartmentalizing protease. Cell **92**, 367–380
4 Voges, D., Zwickl, P. and Baumeister, W. (1999) The 26S proteasome: a molecular machine designed for controlled proteolysis. Annu. Rev. Biochem. **68**, 1015–1068
5 Deveraux, Q., Ustrell, V., Pickart, C. and Rechsteiner, M. (1994) A 26S protease subunit that binds ubiquitin conjugates. J. Biol. Chem. **269**, 7059–7061
6 Deveraux, Q., van Nocker, S., Mahaffey, D., Vierstra, R. and Rechsteiner, M. (1995) Inhibition of ubiquitin-mediated proteolysis by the *Arabidopsis* 26S protease subunit S5a. J. Biol. Chem. **270**, 29660–29663
7 Haracska, L. and Udvardy, A. (1995) Cloning and sequencing a non-ATPase subunit of the regulatory complex of the *Drosophila* 26S protease. Eur. J. Biochem. **231**, 720–725
8 Haracska, L. and Udvardy, A. (1997) Mapping the ubiquitin-binding domains in the p54 regulatory complex subunit of the *Drosophila* 26S protease. FEBS Lett. **412**, 331–336
9 Van Nocker, S., Deveraux, Q., Rechsteiner, M. and Vierstra, R. D. (1996) *Arabidopsis* MBP1 gene encodes a conserved ubiquitin recognition component of the 26S proteasome. Proc. Natl. Acad. Sci. U.S.A. **93**, 856–860
10 Van Nocker, S., Sadis, S., Rubin, D. M., Glickman, M., Fu, H., Coux, O., Wefes, I., Finley, D. and Vierstra, R. D. (1996) The multiubiquitin-chain-binding protein Mcb1 is a component of the 26S proteasome in *Saccharomyces cerevisiae* and plays a nonessential, substrate-specific role in protein turnover. Mol. Cell. Biol. **11**, 6020–6028
11 Wenzel, T. and Baumeister, W. (1995) Conformational constrains in protein degradation by the 20S proteasome. Nat. Struct. Biol. **2**, 199–204
12 Löwe, J., Stock, D., Jap, B., Zwickl, P., Baumeister, W. and Huber, R. (1995) Crystal structure of the 20S proteasome from the archeon *T. acidophilum* at 3.4 Å resolution. Science **268**, 533–539
13 Groll, M., Ditzel, L., Löwe, J., Stock, D., Bochtler, M., Bartunik, H. D. and Huber, R. (1997) Structure of the 20SA proteasome from yeast at 2.4 Å resolution. Nature (London) **386**, 463–471
14 Groll, M., Bajorek, M., Köhler, A., Moroder, L., Rubin, D. M., Huber, R., Glickman, M. H. and Finley, D. (2000) A gated channel into the proteasome core particle. Nat. Struct. Biol. **7**, 1062–1067
15 Braun, B. C., Glickman, M., Kraft, R., Dahlman, B., Kloetzel, P.-M., Finley, D. and Schmidt, M. (1999) The base of the proteasome regulatory particle exhibits chaperone-like activity. Nat. Cell Biol. **1**, 221–226
16 Strickland, E., Hakala, K., Thomas, P. J. and DeMartino, G. N. (2000) Recognition of misfolding proteins by PA700, the regulatory subcomplex of the 26S proteasome. J. Biol. Chem. **275**, 5565–5572
17 Dubiel, W., Ferrell, K., Pratt, G. and Rechsteiner, M. (1992) Subunit 4 of the 26S protease is a member of a novel eukaryotic ATPase family. J. Biol. Chem. **267**, 22699–22702
18 Dubiel, W., Ferrell, K. and Rechsteiner, M. (1995) Subunits of the regulatory complex of the 26S proteasome. Mol. Biol. Rep. **21**, 27–34
19 DeMartino, G. N., Moomaw, C. R., Zagnitko, O. P., Proske, R. J., Ma, C. P., Afendis, S. J., Swaffield, J. C. and Slaughter, C. A. (1994) PA700, an ATP-dependent activator of the 20S proteasome, is an ATPase-containing multiple members of a nucleotide-binding protein family. J. Biol. Chem. **269**, 20878–20884
20 Glickman, M. H., Rubin, D. M., Fried, V. A. and Finley, D. (1998) The regulatory particle of the *Saccharomyces cerevisiae* proteasome. Mol. Cell. Biol. **18**, 3149–3162
21 Hoelzl, H., Kapelari, B., Kellermann, J., Seemüller, E., Sümegi, M., Udvardy, A., Medalia, O., Sperling, J., Müller, S. A., Engel, A. and Baumeister, W. (2000) The regulatory complex of *Drosophila melanogaster* 26S proteasomes: subunit composition and localization of a deubiquitylating enzyme. J. Cell Biol. **150**, 119–129
22 Rubin, D. M., Glickman, M. H., Larsen, C. N., Dhruvakumar, S. and Finley, D. (1998) Active site mutants in the six regulatory particle ATPases reveal multiple roles for ATP in the proteasome. EMBO J. **17**, 4909–4919
23 Girod, P.-A., Fu, H., Zryd, J.-P. and Vierstra, R. D. (1999) Multiubiquitin chain binding subunit MCB1 (RPN10) of the 26S proteasome is essential for developmental progression in *Physcomitrella patens*. Plant Cell **11**, 1457–1471
24 Wilkinson, C. R. M., Ferrell, K., Penney, M., Wallace, M., Dubiel, W. and Gordon, C. (2000) Analysis of a gene encoding Rpn10 of the fission yeast proteasome reveals that the polyubiquitin-binding site of this subunit is essential when Rpn12/Mts3 activity is compromised. J. Biol. Chem. **275**, 15182–15192
25 Lam, Y. A., DeMartino, G. M., Pickart, C. M. and Cohen, R. E. (1997) Specificity of a ubiquitin isopeptidase in the PA700 regulatory complex of 26S proteasomes. J. Biol. Chem. **272**, 28438–28446
26 Papa, F. R., Amerik, A. Y. and Hochstrasser, M. (1999) Interaction of the Doa4 deubiquitinating enzyme with the yeast 26S proteasome. Mol. Biol. Cell **10**, 741–756
27 Eytan, E., Armon, T., Heller, H., Beck, S. and Hershko, A. (1993) Ubiquitin C-terminal hydrolase activity associated with the 26S protease complex. J. Biol. Chem. **268**, 4668–4674
28 Ferrell, K., Wilkinson, C. R. M., Dubiel, W. and Gordon, C. (2000) Regulatory subunit interactions of the 26S proteasome, a complex problem. Trends Biochem. Sci. **25**, 83–88
29 Udvardy, A. (1993) Purification and characterization of a multiprotein component of the *Drosophila* 26S proteolytic complex. J. Biol. Chem. **268**, 9055–9062
30 Hartinger, J., Stenius, K., Hogemann, D. and Jahn, R. (1996) 16BAC/SDS-PAGE: a two dimensional gel electrophoresis system suitable for the separation of integral membrane proteins. Anal. Biochem. **240**, 126–133
31 Shulman, M., Wide, C. D. and Köhler, G. (1978) A better cell line for making hybridomas secreting specific antibodies. Nature (London) **276**, 269–271
32 Adrian, M., Dubochet, J., Fuller, S. D. and Harris, J. R. (1998) Cryo-negative staining. Micron **29**, 145–160
33 Baumeister, W., Dahlmann, B., Hegerl, R., Kopp, F., Kuehn, L. and Pfeifer, G. (1988) Electron microscopy and image analysis of the multicatalytic proteinase. FEBS Lett. **241**, 239–245
34 van Heel, M. and Frank, J. (1981) Use of multivariate statistics in analysing the images of biological macromolecules. Ultramicroscopy **6**, 187–194
35 Richmond, C., Gorbea, C. and Rechsteiner, M. (1997) Specific interactions between ATPase subunits of the 26S protease. J. Biol. Chem. **272**, 13403–13411
36 Gorbea, C., Taillandier, D. and Rechsteiner, M. (2000) Mapping subunit contacts in the regulatory complex of the 26S proteasome: S2 and S5b form a tetramer with ATPase subunits S4 and S7. J. Biol. Chem. **275**, 875–882
37 Russell, S. J., Reed, S. H., Huang, W., Friedberg, E. C. and Johnston, S. (1999) The 19S regulatory complex of the proteasome functions independently of proteolysis in nucleotide excision repair. Mol. Cell **3**, 687–695
38 Mason, G. G. F., Murray, R. Z., Pappin, D. and Rivett, J. A. (1998) Phosphorylation of ATPase subunits of the 26S proteasome. FEBS Lett. **430**, 269–274
39 Verma, R., Chen, S., Feldman, R., Schieltz, D., Yates, J., Dohmen, J. and Deshaies, R. J. (2000) Proteasomal proteomics: identification of nucleotide-sensitive proteasome-interacting proteins by mass spectrometric analysis of affinity-purified proteasomes. Mol. Biol. Cell **11**, 3425–3439
40 Davy, A., Bello, P., Thierry-Mieg, N., Vaglio, P., Hitti, J., Doucette-Stamm, L., Thierry-Mieg, D., Reboul, J., Boulton, S., Walhout, A. J. M., Coux, O. and Vidal, M. (2001) A protein-protein interaction map of the *Caenorhabditis elegans* 26S proteasome. EMBO Rep. **2**, 821–828
41 Cagney, G., Uetz, P. and Fieéds, S. (2001) Two-hybrid analysis of the *Saccharomyces cerevisiae* 26S proteasome. Physiol. Genomics **7**, 27–34
42 Fu, H., Reis, N., Lee, Y., Glickman, M. H. and Vierstra, R. D. (2001) Subunit interaction maps for the regulatory particle of the 26S proteasome and the COP9 signalosome. EMBO J. **20**, 7096–7107

Received 19 October 2001/28 March 2002; accepted 11 April 2002
Published as BJ Immediate Publication 11 April 2002, DOI 10.1042/BJ20011520